Mesoporous silica nanoparticle based controlled release, drug delivery, and biosensor systems

Brian G. Trewyn, Supratim Giri, Igor I. Slowing and Victor S.-Y. Lin*

Received (in Cambridge. UK) 5th February 2007, Accepted 2nd March 2007
First published as an Advance Article on the web 20th March 2007
DOI: 10.1039/b701744h

Recent advancements in controlling the surface properties and particle morphology of the structurally defined mesoporous silica materials with high surface area (>700 m^2 g^{-1}) and pore volume (>1 cm^3 g^{-1}) have significantly enhanced their biocompatibility. Various methods have been developed for the functionalization of both the internal pore and exterior particle surfaces of these silicates with a tunable pore diameter ranging from 2 to 30 nm and a narrow pore size distribution. Herein, we review the recent research progress on the design of functional mesoporous silica materials for stimuli-responsive controlled release delivery of pharmaceutical drugs, genes, and other chemicals. Furthermore, the recent breakthroughs in utilizing these nanoscale porous materials as sensors for selective detections of various neurotransmitters and biological molecules are summarized.

Introduction

Since the discovery of MCM-41 material in 1992 by researchers at Mobil,[1] there has been a great deal of research done on the morphology control and surface functionalization

Department of Chemistry and U.S. DOE Ames Laboratory, Iowa State University, Ames, Iowa, 50011, USA. E-mail: vsylin@iastate.edu; Tel: +01-515-294-3135

Brian G. Trewyn

Brian G. Trewyn received his BSc in Chemistry and Micro-?biology of the University of Wisconsin-La Crosse in 2000 and his PhD from Iowa State University in the Spring of 2006. He joined the Department of Chemistry at Iowa State University as an assistant scientist and is currently working with Prof. Victor Lin. His research centers on biological applications of mesoporous silica nanomaterials.

Supratim Giri

Supratim Giri received his BSc in chemistry from Presidency College Kolkata, India in 1997 and MSc in chemistry from Indian Institute of Technology, Kanpur, India in 2002. He is currently a PhD candidate in Victor Lin's research group in the Department of Chemistry at Iowa State University. His research focuses on the development of magnetic nanoparticle based stimuli-responsive delivery systems.

Igor I. Slowing

Igor I. Slowing received his License degree in Chemistry from San Carlos University in Guatemala in 1995. He is currently a PhD candidate in Victor Lin's research group at Iowa State University. He studies biological applications of mesoporous silica nanoparticles.

Victor S.-Y. Lin received his PhD from the University of Pennsylvania in the end of 1996. After working as a Skaggs postdoctoral fellow at the Scripps Research Institute,

Victor S.-Y. Lin

he joined the faculty at Iowa State University in the Fall of 1999. He is currently a Professor of Chemistry at Iowa State University and an assistant program director of the Chemical and Biological Sciences program at the U.S. DOE Ames Laboratory. His research centers on the design of functional nanoporous materials for selective catalysis and biotechnological applications, such as biosensor design, drug delivery, and gene transfection.

of a variety of mesoporous silica materials, such as MCM-, SBA-, MSU-, KSW- and FSM-type of mesoporous silicas.[2] A major goal of these research efforts was to functionalize these structurally well-defined mesoporous materials with tunable pore diameter (2–30 nm), narrow pore size distribution, and high surface area (>700 m^2 g^{-1}) for various applications in adsorption, catalysis, separation, delivery, and sensing. This Feature Article summarizes the recent endeavors of our laboratory and related works by other investigators on the development of mesoporous silica-based systems for controlled release delivery of drugs,[3] biocides, nutrients, genes,[4] or even proteins,[5] and for the selective detections of neurotransmitters[6,7] and other biological molecules.

Mesoporous silica-based controlled release systems

An important prerequisite for designing an efficient delivery system is the ability to transport the desired guest molecules to the targeted site and release the cargo in a controlled manner.[8] Premature release of guest molecules[9] presents a challenging problem. For example, delivery of toxic anti-tumor drugs require "zero release" before reaching the targeted cells or tissues. However, the release mechanism of many current biodegradable polymer-based drug delivery systems relies on the hydrolysis-induced erosion of the carrier structure. The release of encapsulated compounds usually takes place immediately upon dispersion of these composites in water. Also, such systems typically require the use of organic solvents for drug loading, which could sometimes trigger undesirable modifications of the structure and/or function of the encapsulated molecules, such as protein denaturation and aggregation. In contrast, the surface functionalized mesoporous silica materials offer several unique features, such as stable mesoporous structures, large surface areas, tunable pore sizes and volumes, and well-defined surface properties for site-specific delivery and for hosting molecules with various sizes, shapes, and functionalities. The unique hexagonally ordered pore structures of the MSNs offer an important advantage for drug delivery over those of porous hollow silica nanoparticles. Porous hollow nanoparticles have pores connected to one large reservoir, where the encapsulated drug molecules could be released through any of these interconnected pores.[10–12] Therefore, a perfect capping of all of the pore openings is required to achieve "zero premature release". However, in the case of our MSN, where the pores are independent parallel channels without any interconnection, each pore only has two openings. A "zero premature release" system could still be generated in a situation of imperfect capping, as long as both of the openings of a single mesopore are capped.

Non-functional MCM-41 and morphology controlled release

During the past five years, there have been several examples of MCM-41 type silicas used for drug delivery and controlled release. For example, Ibuprofen was loaded into MCM-41 materials with different pore sizes and studied the release in a simulated body fluid.[13] This report demonstrated that the unique MCM-41 mesoporous structure with channel-like pores packed in a hexagonal fashion could be used for loading of a large quantity of drugs, while controlling the rate of release of drugs.

To investigate how the pore and particle morphology of mesoporous silica materials would impact the controlled release properties, we developed a room-temperature ionic liquid (RTIL) templated mesoporous silica nanoparticle (MSN) system for controlled release of antimicrobial agents.[14] We synthesized four different RTILs through previously published methods (Fig. 1(a)). Subsequently, a series of RTIL-MSN materials with various particle morphologies including spheres, ellipsoids, rods, and tubes, was prepared with these RTILs, which were utilized as templates. By changing the RTIL template, the pore morphologies were tuned from the MCM-41 type of hexagonal mesopores to rotational Moiré type of helical channels, and to wormhole-like porous structures. We investigated controlled release of the pore-encapsulated ionic liquids by measuring the antibacterial effect on *Escherichia coli* K12 (Fig. 1(b)).[14]

First, we measured the antibacterial activities of two RTIL in homogeneous solution, and compared with those of two RTIL-MSNs, one spherical with hexagonal mesopores and the other tubular with wormhole mesopores (Fig. 2(a) and (b)), at 37 °C in *E. coli* cultures. While both the RTILs displayed very similar antibacterial activities, the spherical, hexagonally

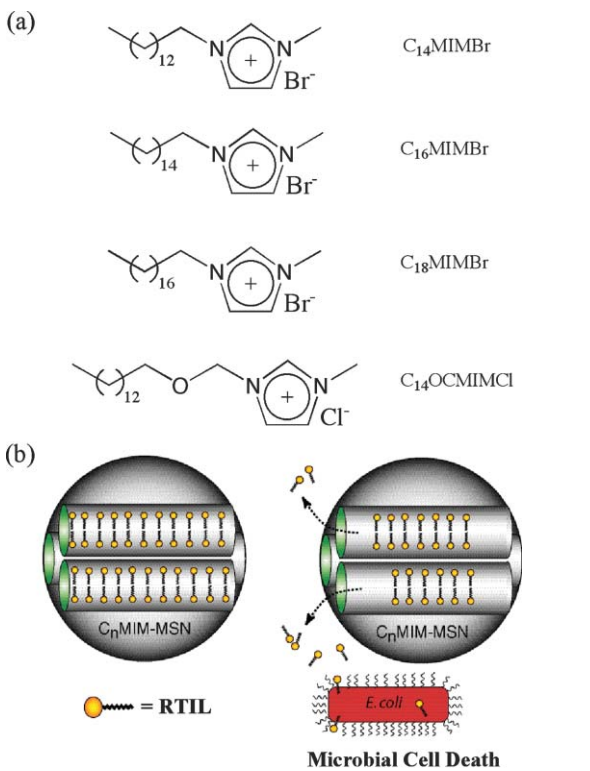

Fig. 1 (a) Chemical structures of 1-tetradecyl-3-methylimidazolium bromide (C_{14}MIMBr), 1-hexadecyl-3-methylimidazolium bromide (C_{16}MIMBr), 1-octadecyl-3-methylimidazolium bromide (C_{18}MIMBr), and 1-tetradecyloxymethyl-3-methylimidazolium chloride (C_{14}OCMIMCl). (b) Schematic representation of the controlled release process of C_nMIM-MSN and its antibacterial activity against *E. coli*. Reprinted with permission from ref. 14. Copyright 2004, American Chemical Society.

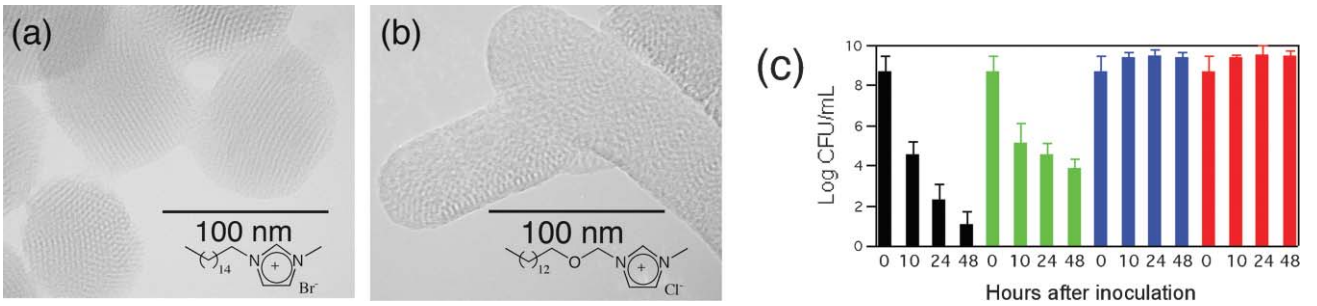

Fig. 2 Transmission electron micrographs of C_nMIM-MSN materials. (a) C_{16}MIM-MSN and (b) C_{14}OCMIM-MSN. These micrographs were obtained from a Phillips CM30 TEM operated at 300 kV. (c) Histogram of the antibacterial activity of C_nMIM-MSNs against *E. coli K12* at 37 °C. Four samples were measured at 37 °C: C_{16}MIM-MSN (black bars), C_{14}OCMIM-MSN (green bars), RTIL-removed C_{16}MIM-MSN (blue bars), and blank control (no silica material) (red bars). Reprinted in part with permission from ref. 14. Copyright 2004, American Chemical Society.

mesopore RTIL-MSN exhibited a superior antibacterial activity (1000-fold) to that of the tubular, wormhole RTIL-MSN (Fig. 2(c)).[14] This result was attributed to the fact that the rate of RTIL release *via* diffusion from the parallel hexagonal channels would be faster than that of the disordered wormhole pores. This work categorically demonstrated the essential role of the morphology of mesoporous silica nanomaterials on controlled release behavior.

Stimuli-responsive controlled release from inorganically functionalized MSNs

As mentioned previously, it is highly desirable to design delivery systems that can respond to external stimuli and release the guest molecules at specific sites. To achieve this goal, our group developed a series of stimuli-responsive, MCM-41 type mesoporous silica nanoparticle-based controlled release delivery system.[3,15,16] As depicted in Fig. 3, the mesopores loaded with guest molecules were capped by CdS nanoparticles *via* a chemically cleavable disulfide linkage to the MSN surface. Being physically blocked, guest molecules were unable to leach out from the MSN host, thus preventing any premature release. The release was triggered by exposing the capped MSNs to chemical stimulation[3] that could cleave the disulfide linker, thereby removing the nanoparticle caps and releasing the pore-entrapped guest molecules.

We first prepared a mercaptopropyl-derivatized mesoporous silica nanosphere material (thiol-MSN) following our reported co-condensation method.[6] The surfactant-removed thiol-MSN material was treated with 2-(pyridyldisulfanyl)ethylamine[17] to obtain a chemically labile disulfide bond-containing, amine-functionalized MSN material (Linker-MSN) (Fig. 3). Scanning electron microscopy (SEM) revealed the spherical morphology of the Linker-MSN with an average particle size of 200 nm (Fig. 4(a) and (b)). The MCM-41 type of hexagonally packed mesoporous structure of this material was confirmed by transmission electron microscopy (TEM) (Fig. 4(c) and (e)). Nitrogen sorption studies of the Linker-MSN revealed high surface area (>900 $m^2\ g^{-1}$) and a narrow pore size distribution (average pore size = 2.3 nm).

To demonstrate that the porous channels of mesoporous silica can serve as a reservoir for biomolecules, our Linker-MSN material was used as a chemically inert host to soak up aqueous solutions of vancomycin and ATP. To block the mesopores, we synthesized mercaptoacetic acid-coated CdS nanocrystals[18] (2.0 nm size) as chemically removable caps (Fig. 4(d) and (f)). As shown in Fig. 3, in the presence of drug

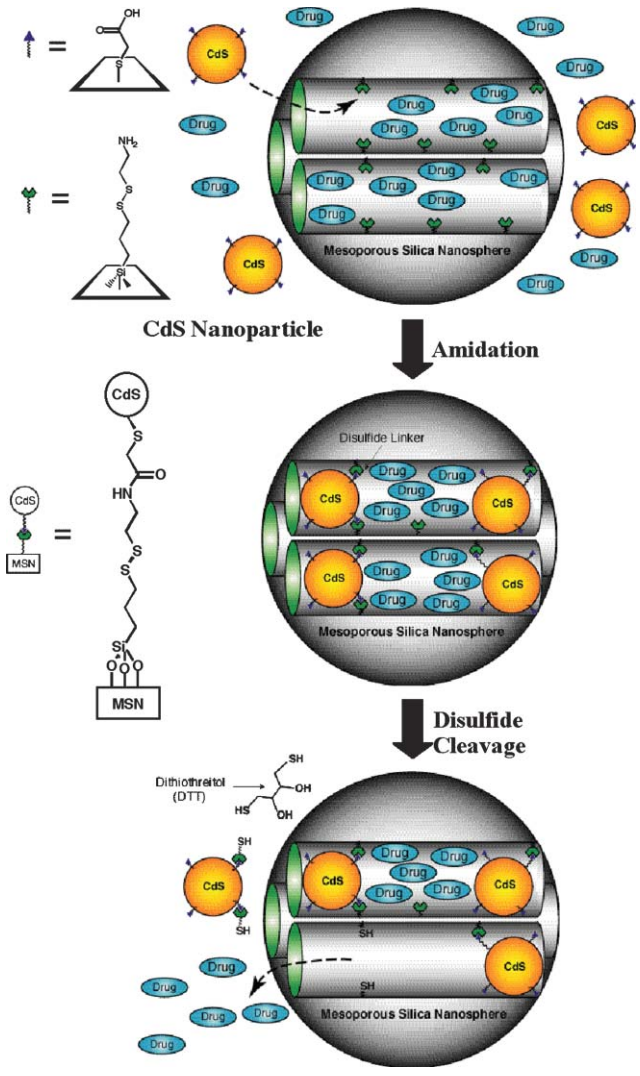

Fig. 3 Schematic representation of the CdS nanoparticle-capped MSN-based drug/neurotransmitter delivery system. The controlled release mechanism of the system is based on chemical reduction of the disulfide linkage between the CdS nanoparticles and MSN. Reprinted in part with permission from ref. 3. Copyright 2003, American Chemical Society.

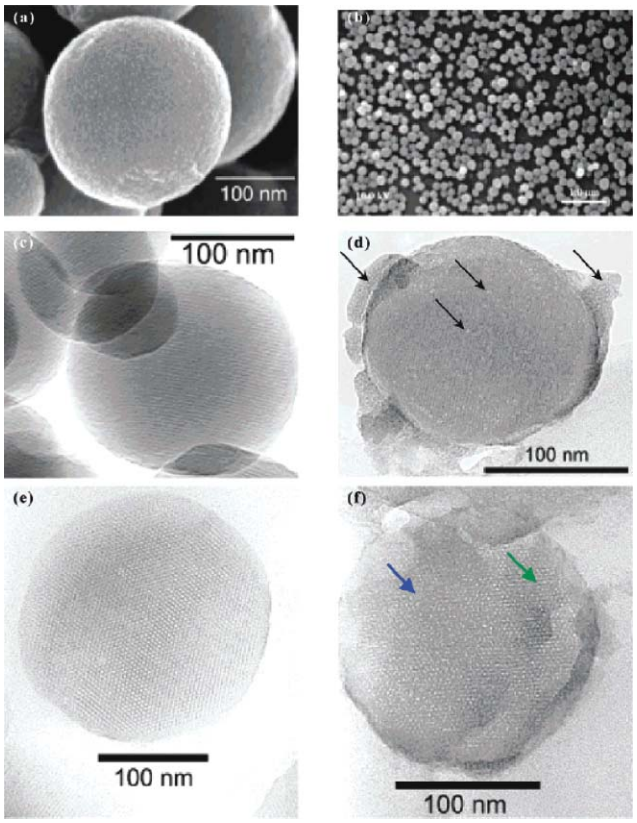

Fig. 4 SEM (a, b) and TEM (300 kV) micrographs of the Linker-MSN (c, e). The TEM micrographs (d, f) of the CdS-capped MSN clearly exhibit aggregations of CdS nanoparticles on the exterior surface of MSN material represented by dots in the areas indicated by black arrows in (d). The TEM micrographs (d–f) were measured on ultramicrotomed samples with section thickness of 60–80 nm. Reprinted with permission from ref. 3. Copyright 2003, American Chemical Society.

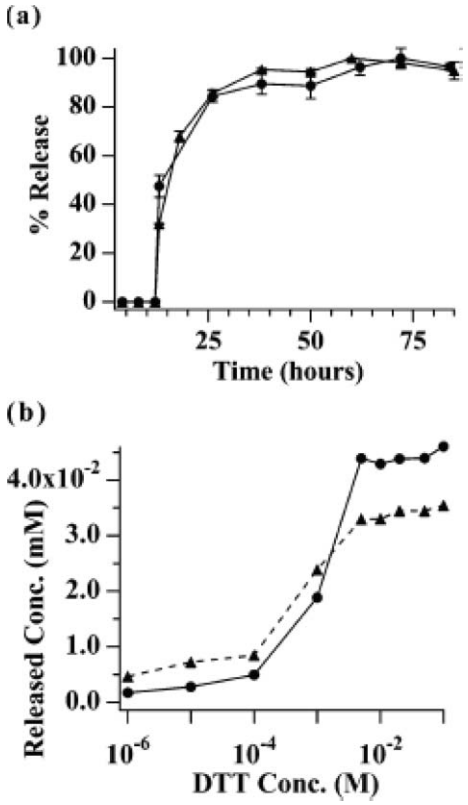

Fig. 5 The DTT-induced release profiles of vancomycin (solid circles) and ATP (solid triangles) from the CdS-capped MSN system: (a) percentage release over time. (b) The DTT concentration-dependent releases. Released analyte concentrations were measured with CdS-MSNs (2.3 mg) in pH 7.4 PBS buffers (0.8 mL) after 24 h of the DTT additions. Reprinted with permission from ref. 3. Copyright 2003, American Chemical Society.

molecules (ATP or vancomycin) the water-soluble CdS nanocrystals were covalently captured by the Linker-MSN through the formation of an amide bond. The loading efficiency of vancomycin and ATP was found to be 83.9 and 30.3 mol%, respectively.

To establish the fact that the resulting disulfide linkages between the MSNs and the CdS nanoparticle caps are indeed *chemically labile* and can be cleaved by various disulfide reducing agents, we applied dithiothreitol (DTT) and mercaptoethanol (ME) as chemical stimuli to observe the release of vancomycin/ATP.[3] Our CdS-capped MSN drug/neurotransmitter delivery system showed no premature release in PBS (10 mM, pH 7.4) over a period of 12 h in the absence of disulfide reducing agent suggesting an excellent capping efficiency as shown in Fig. 5(a).[3] Addition of disulfide-reducing agents, such as DTT and ME, triggered, a rapid release of drug/neurotransmitter. The results of the addition of 18.5 mM DTT are shown in Fig. 5(a).[3] The majority (85%) of the total molecules were released within the initial 24 h following similar diffusional kinetic profiles for both vancomycin and ATP. Furthermore, in both cases, the amount of drug release after 24 h showed similar DTT concentration dependences (Fig. 5(b)), indicating the rate of release is dictated by the rate of removing the CdS caps.[3]

We also demonstrated the biocompatibility and the utility of our CdS capped MSN delivery systems *in vitro* with neuroglial cells (astrocytes).[3] It is known that ATP evokes a receptor-mediated increase in intracellular calcium in astrocytes,[19] which is an important regulatory mechanism for many intercellular communications and cooperative cell activities.[20] Neuron-free astrocyte type-1 cells were cultured in the presence of surface immobilized, CdS capped MSNs with encapsulated ATP molecules. Cells were also loaded with Ca^{2+} chelating fluorescent dye (Fura-2). Upon perfusion application of mercaptoethanol (ME), we observed a pronounced increase in intracellular $[Ca^{2+}]_i$. The application of ME triggered the release of ATP molecules from MSNs and hence giving rise to the corresponding ATP receptor mediated increase in intracellular calcium concentration.[3]

To introduce site-directing capability to the MSN-based delivery system, we designed a MSN material capped with superparamagnetic iron oxide (Fe_3O_4) nanoparticles.[15] In addition to having a stimuli-responsive controlled release property, we have demonstrated that the magnetic nanoparticle-capped MSN can be attracted to specific site of interest under a magnetic field. The system consists of rod-shaped MSNs functionalized with 3-(propyldisulfanyl)propionic acid to give "Linker-MSNs" that have an average particle size of 200 nm × 80 nm (length × width) and an average pore

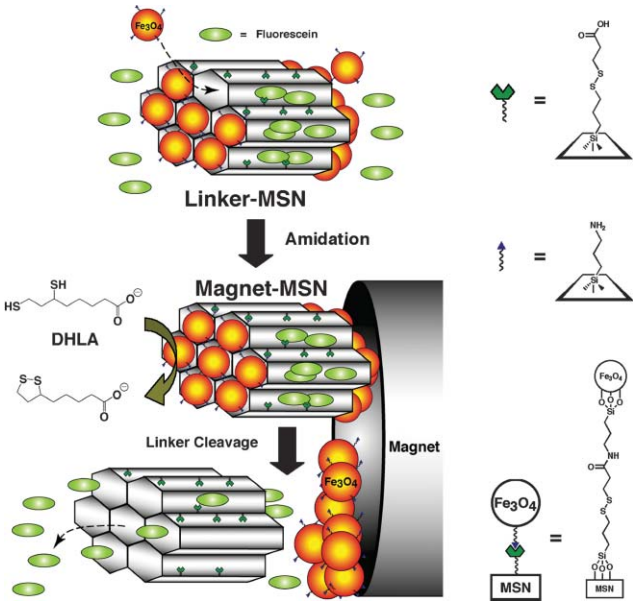

Fig. 6 Schematic of the stimuli-responsive delivery system (Magnet-MSN) based on mesoporous silica nanorods capped with superparamagnetic iron oxide nanoparticles. Reprinted with permission from ref. 15. Copyright 2005, Wiley Publishing Company.

diameter of 3.0 nm. As a proof of principle, fluorescein was used as the guest molecule. The openings of the mesopores of the fluorescein-loaded Linker-MSN were covalently capped *in situ* through an amidation of the 3-(propyldisulfanyl)propionic acid functional groups bound at the pore surface with 3-aminopropyltriethoxysilyl-functionalized superparamagnetic iron oxide (APTS-Fe_3O_4) nanoparticles as shown in Fig. 6.[15]

To demonstrate that the entire Fe_3O_4-capped MSN (Magnet-MSN) carrier system can be magnetically directed to a site of interest where the controlled release can take place under a magnetic field, two cuvettes were charged with fluorescein-loaded Magnet-MSNs in PBS solution (100 mM, pH 7.4). As illustrated in Fig. 7(a), the Magnet-MSNs were attracted to the walls of the cuvettes closest to the tips of magnets.[15] Dithiothreitol was added to one of the two cuvettes (left) for the release experiment, while the other cuvette (right) served as a control. After 12 h and 4 days (Fig. 7(b) and (c), respectively[4]), green fluorescence was clearly observed in the solution to which DTT was added whereas no fluorescence could be observed from the control solution.[15] These results indicate that fluorescein molecules were indeed released from the Magnet-MSNs by the introduction of the disulfide-reducing trigger DTT. The kinetics of the controlled release of fluorescein by cell-produced antioxidant and disulfide reducing agent such as dihydrolipoic acid (DHLA) and dithiothreitol (DTT), respectively, showed similar behavior as in the CdS capped MSN case (Fig. 7(d) and (e)).[3]

To investigate the endocytosis and biocompatibility of this system, HeLa (human cervical cancer) cells were incubated overnight with Magnet-MSNs to allow the endocytosis of Magnet-MSNs.[15] The cells that took up Magnet-MSNs were magnetically separated from those that did not. The isolated cells were treated with nucleus staining blue-fluorescent dye 4′,6-diamidino-2-phenylindole (DAPI) dye in PBS solution (100 mM, pH 7.4) and placed in a cuvette. When a magnet was moved along the side of the cuvette, the blue-fluorescent HeLa cells were clearly seen to move across the cuvette toward the magnet (Fig. 8(a)–(c)) indicating that the Magnet-MSNs were indeed endocytosed by HeLa cells.[15] To further confirm the endocytosis of Magnet-MSNs, these HeLa cells were examined

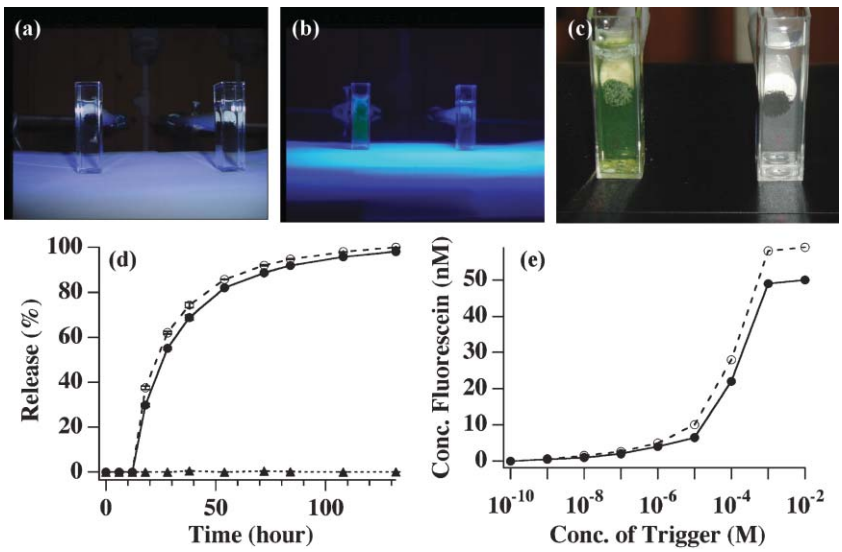

Fig. 7 (a–c) Photographs of two cuvettes charged with fluorescein-loaded Magnet-MSNs (50.0 mg each) dispersed in 3.00 mL of PBS solution (100.0 mm, pH 7.4). In the left cuvette DTT (48.5 mg) was added. (d) Controlled release of fluorescein from Magnet-MSNs (13.0 mg) in 3.00 mL of PBS solution (100.0 mm, pH 7.4) triggered by 0.1 mm DHLA (solid circle) or DTT (blank circle). No noticeable release was observed in the absence of a reductant (solid triangle). (e) The dependence of the release of fluorescein from Magnet-MSNs on the concentration of the reductant, measured 72 h after the addition of DHLA or DTT. Reprinted with permission from ref. 15. Copyright 2005, Wiley Publishing Company.

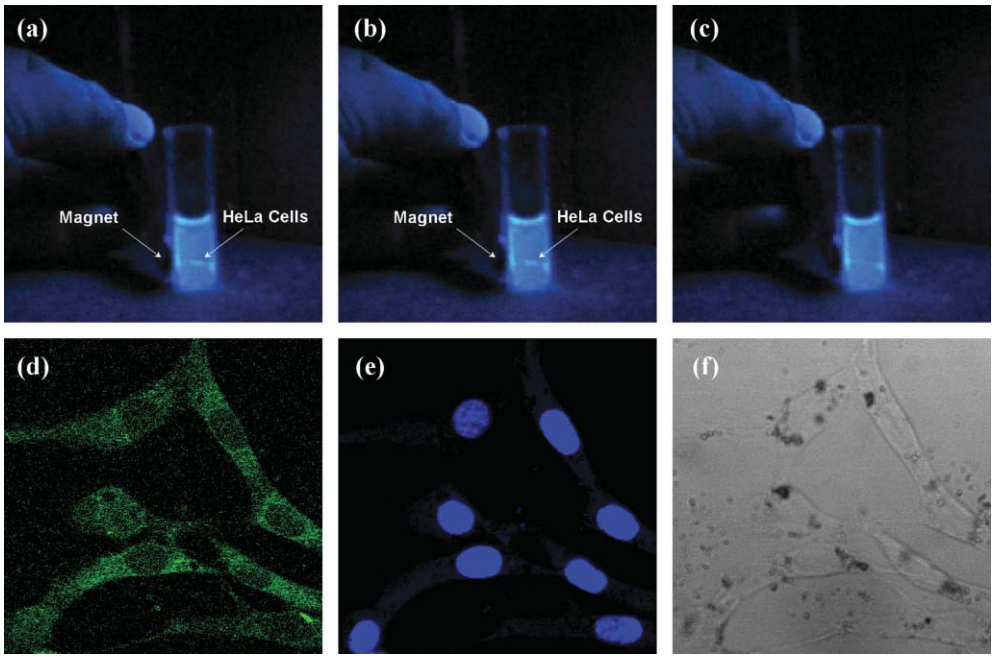

Fig. 8 (a)–(c)) Single frames of photographs of HeLa cells with Fe_3O_4-capped fluorescein-loaded MSNs traveling across the cuvette, propelled by magnetic force. (d)–(f) Fluorescence confocal micrographs of HeLa cells after 10 h incubation with Fe_3O_4-capped fluorescein-loaded MSNs: (d) cells excited at 494 nm; (e) cells excited in the UV region; (f) a pseudo-brightfield image, where dark aggregations of Magnet-MSNs can be clearly observed. Reprinted with permission from ref. 15. Copyright 2005, Wiley Publishing Company.

by confocal fluorescence microscopy (Fig. 8(d)–(f)). The observed green fluorescence (Fig. 8(d)) strongly indicated that the mesopore-encapsulated fluorescein molecules were released inside the cells. As previously reported, cancer cell lines express significant amounts of DHLA,[21] we attributed the efficient intracellular release of fluorescein to the high intracellular concentration of DHLA serving as the trigger.[15]

Stimuli-responsive controlled release from organically functionalized MSNs

While we demonstrated chemically stimulated controlled release from MSNs in an aqueous environment, Tanaka and co-workers demonstrated the ability of coumarin-modified mesoporous silica being used as a photocontrolled reversible guest molecule release vehicle in organic solvent.[22] They showed that the uptake, storage, and release of organic molecules using coumarin-modified MCM-41 can be regulated through photocontrolled and reversible intermolecular dimerization. The coumarin was covalently attached to the MCM-41 pore walls by post-synthesis grafting and the pores were loaded with cholestane, a steroid, followed by photodimerization of the coumarin by exposure to light greater than 310 nm. The resulting photodimerization led to the isolation of pores by blocking the pore entrance with cyclobutane dimers spanning the pore diameter. The cholestane loaded photodimerized material was then exposed to UV light with a wavelength of 250 nm to cleave the cyclobutane rings of the coumarin dimers and the subsequent release of the stored cholestane molecules was observed. The publication was the first to demonstrate a photocontrolled release of guest molecules from MCM-41 material by reversible photoresponsive dimerization techniques.

In addition to the utilization of inorganic nanoparticles as caps, we have demonstrated that large organic molecules can also be used to modify the surface properties of mesoporous silicas to achieve controlled release.[4] Our report was also the first uptake study of MCM-41 type mesoporous silicas into eukaryotic cells. We described the synthesis of thiol-unctionalized MCM-41, and the covalent attachment of second generation (G2) PAMAM dendrimer to the surface of a MCM-41 type mesoporous silica nanosphere (MSN). The G2-PAMAM-capped MSN (G2-MSN) was used to complex with plasmid DNA (pEGFP-C1) that codes for enhanced green fluorescent protein. We investigated the gene transfection efficacy, uptake mechanism, and biocompatibility of the G2-MSN with astrocytes, HeLa, and Chinese hamster ovarian (CHO) cells (Fig. 9(a)).[4] Through gel electrophoresis it was determined that the G2-MSN could bind with plasmid DNA to form stable DNA-MSN complexes at weight ratios larger than 1 : 5. By introducing varying ratios of restriction endonucleases to the complex, we also showed that this DNA-MSN complex protects the plasmid DNA from enzymatic cleavage. Transfection efficacy was demonstrated by incubating the DNA-MSN complex with cells and measuring the expression of GFP by flow cytometry and the results were compared to other commercially available transfection reagents. We concluded that our material had better transfection efficiency than all tested commercial transfection reagents. Fluorescence confocal microscopy clearly illustrated that the G2-MSN, entered the cytoplasm of neural glia cells. Transmission electron micrographs of post-transfection cells also provided direct evidence that a large number of G2-MSN-DNA complexes were endocytosed by all three cells types (Fig. 9(b) and (c)).[4] Many subcellular organelles, such as mitochondria

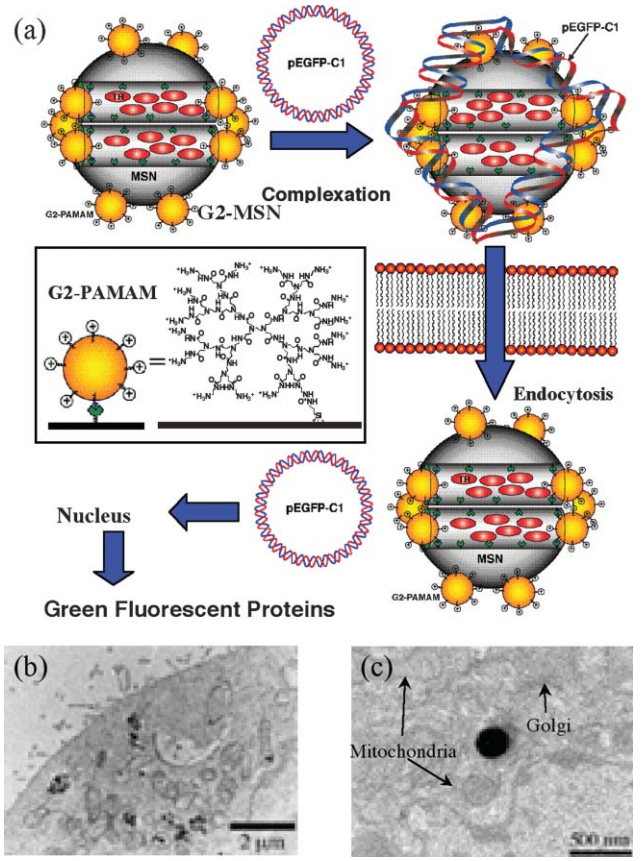

Fig. 9 (a) Schematic representation of a non-viral gene transfection system based on a Texas Red™ (TR)-loaded, G2-PAMAM dendrimer-capped MSN material complexed with an enhanced green fluorescence protein (*Aequorea victoria*) plasmid DNA (pEGFP-C1). (b and c). TEM micrographs of G2-MSN-DNA complexes (black dots) endocytosed by HeLa (b), and astrocyte (c) cells. Subcellular organelles, *e.g.*, mitochondria and Golgi, were observed. Reprinted in part with permission from ref. 4. Copyright 2004, American Chemical Society.

and Golgi, were observed with MSNs nearby, strongly suggest that the MSNs were not cytotoxic *in vitro*.

Mou and co-workers[23,24] studied the mechanism of cellular uptake of fluorescein labeled MSNs in 3T3-L1 fibroblast cells and mesenchymal stem cells, showing that the endocytosis of the material was time- and concentration-dependent and clathrin mediated. They also demonstrated that the MSNs were also able to escape the endolysosomal vesicles and showed no cytotoxicity.

Recently we published a communication reporting the effects of surface functionalization of MSN on endocytosis of human cancer cells.[25] We functionalized MSN with organic groups of different charge profiles and investigated the mechanism and efficiency of endocytosis. We discovered that MSN functionalized with fluorescein and folic acid were endocytosed *via* a clathrin-pitted mechanism. We also discovered that the more negatively charged MSNs were able to escape from endosomes while the MSNs with more positive ζ-potentials remained trapped within endosomes after 6 h.

Apart from the chemical stimuli, an efficient electrochemical redox activated system based on mesoporous silica was developed by Zink, Stoddart, and co-workers.[26] The investigators demonstrated a supramolecular nanovalve that can be turned on by redox chemistry (Fig. 10). The mesopores were loaded with $Ir(ppy)_3$, a fluorescent molecule, and contained it by using a pseudorotaxane as a gatekeeper. The opening of the nanovalve was stimulated by the addition of an external reducing agent, which causes the pseudorotaxane to disassemble. Following this publication, Zink and co-workers further developed a reversibly operated nanovalve that can be turned on and off by redox chemistry.[27] The MCM-41 was functionalized with a redox-controllable rotaxane with a moveable molecule, tetracationic cyclophane, which can be induced to move between two different recognition sites. In the ground state the cyclophane prefers to encircle a tetrathiafulvalene (TTF), the functional group near the pore end of the rotaxane and caps the pore. Upon a two-electron oxidation of the TTF group with $Fe(ClO_4)_3$ (to give TTF^{2+}) the cyclophane–TTF interaction is destabilized through coulombic repulsion and the cyclophane travels to the dioxynaphthalene (DNP) group, which is separated from the TTF by an oligoethylene glycol chain. This movement of the cyclophane to the DNP uncaps the pore and allows for the free movement of guest molecules. Reduction of the TTF^{2+} to TTF by ascorbic acid heralds the return of the cyclophane to the TTF and thus recaps of the pore. This was the first report of a reversibly operating nanovalve that can be turned on and off by redox chemistry. The same researchers recently did a comparative study investigating the dependence of the length of the nanovalves and placement of the attachment sites in the MCM-41 relative to the openings of the pores on the release of guest molecules. It was discovered that shorter linkers lead to less leaky nanovalves and the nanovalves were more efficient when they were anchored deep within the pores than when they were anchored near the openings of the pores. However, the variation in the length between the TTF and the DNP sites did not affect the functioning of the nanovalves.[28]

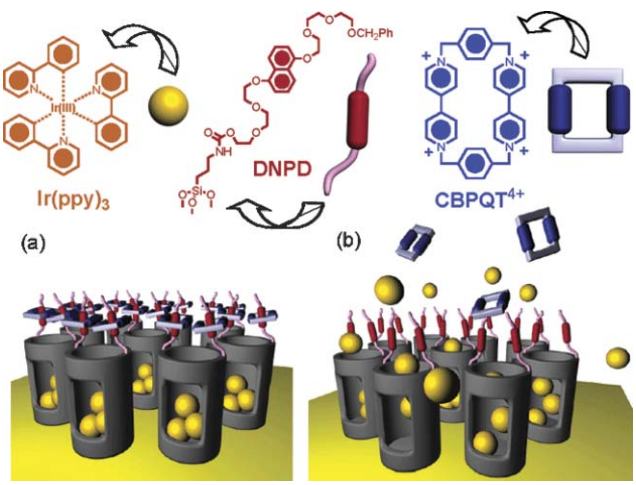

Fig. 10 Graphical representations of operation of nanovalves. (a) The orifices of the nanopores (diameter 2 nm) are covered with pseudorotaxanes (formed between DNPD and $CBPQT^{4+}$) which trap the luminescent $Ir(ppy)_3$ molecules inside the nanopores. (b) Upon their reduction, the $CBPQT^{2+}$ bisradical dications are released and allow the $Ir(ppy)_3$ to escape. Reprinted with permission from ref. 26. Copyright 2004, American Chemical Society.

In addition, Zink, Stoddart, and co-workers reported a slightly different system that the openings of functional MCM-41 are regulated by supermolecules that are controlled by pH and competitive binding.[29,30] In this system different bases with a range of basicities were utilized to deprotonate the dialkylammonium stalk of the nanovalve and disrupt the interaction between the secondary amine on the stalk and the dibenzo[24]crown-8 ring, thus uncapping the pores and releasing the guest molecules. They demonstrated competitive binding release by adding molecules that the dibenzo[24]-crown-8 ring binds stronger to than the tethered dialkyl-ammonium stalk, so opening the nanovalves, and releasing the guest molecules.

Multifunctional mesoporous silicas for biosensor applications

Since the mid 1990s nanomaterials have been increasingly considered as an attractive option for biosensing applications.[31–33] The unique surface properties and the small particle size of these nanoparticle-based sensor systems allow the detection of analytes in microscopic space within individual cells for both *in vivo* and *in vitro* detection.[34] Also, for intracellular detection, nanoparticles represent an advantageous alternative to homogeneous cellular staining dyes due to the fact that, unlike stains, nanoparticles do not suffer from the fluorescent self-quenching and other diffusion-related problems.[35]

Among the different nanoparticle biosensors, enzyme-immobilized nanoparticles have been reported in numerous publications.[36–38] While enzyme-based sensors show great specificity and low concentration detection limits, they suffer from denaturation and inactivation, plus they lack two important characteristics held by mesoporous silicas: *high porosity*, which results in large surface areas available for the immobilization of the sensing molecules, and *optical transparency*, which permits optical detection through the layers of the material. The former property allows for the location of sensing molecules not only on the external surface of the material but also inside of the pores which enables the loading of large amounts of sensing molecules, giving fast responses and low detection limits. Silicate glass obtained by the sol–gel process has been used for biosensing purposes.[39–41] Microporous silica nanoparticles have long been used for the creation of biosensors utilizing drugs, enzymes, antibodies[34,42–44] and DNA[45] as recognition elements. However, pores in sol–gel derived silica lack a high degree of order, which results in nonlinear paths, and consequently slow diffusion of the analytes to the sensing molecules – a fraction of the sensing molecules might even be unreachable – leading to less than optimal response. In contrast to microporous silica, mesoporous silica has much more available surface area due to its larger and more ordered pores. This allows for larger concentrations of accessible receptor molecules, the possibility to detect larger molecules, and a faster diffusion to the sites where the receptors are located, which altogether results in even faster and better response of the sensors.

Proteins have been used largely as active elements for the selectivity of mesoporous silica supported biosensors. For example, mesoporous silica was loaded with glucose oxidase and horseradish peroxidase and used as a sensor for glucose.[46,47] In another study myoglobin and hemoglobin were immobilized in mesoporous silica modified electrodes to be used as a sensor for H_2O_2 and NO_2^-.[48,49] The main reason for using enzymes and proteins as the recognition unit is their high specificity for substrates. However, these biomolecules are relatively expensive and lack long-term chemical stability. To avoid these disadvantages, while maintaining high analyte selectivity, we and other groups have pursued a new approach. Unlike the molecular imprinting approach, we attained the selectivity not by synthesizing size or shape selective recognition receptors, but by controlling the diffusional penetration of analytes into the surface-functionalized mesopores. As described below, new mesoporous silica-based selective sensory systems by using this strategy have been reported.

To introduce a signal transduction mechanism to the mesoporous silica nanoparticle material, we first prepared an *o*-phthalic hemithioacetal (OPTA) functionalized MSNs, which would fluoresce upon reaction with a primary amine.[6] This OPTA-MSN material was further derivatized into a selective sensor system that is able to distinguish between the two similarly sized biogenic molecules, dopamine and glucosamine. We grafted propyl, phenyl and pentafluorophenyl groups to the OPTA-MSNs to manipulate properties, such as hydrophobicity and analyte/selective group interaction. The largest difference in the fluorescence responses to the two analytes was observed in the case of pentafluorophenyl grafted OPTA-MSN. This difference was attributed to the π–π acceptor/donor interactions occurring between the aromatic ring of the dopamine and the pentafluorophenyl groups. In this way we demonstrated that secondary non-covalent interactions can play a significant role in the selectivity of a biosensor.[6]

To develop a biosensor suitable to distinguish between several structurally similar neurotransmitters, such as dopamine, tyrosine and glutamic acid, we exploited the ability of selective functionalization of the exterior and interior surfaces (Fig. 11).[7] The molecular recognition system we have developed was synthesized by first functionalizing the pores with OPTA groups. The exterior surface of OPTA-MSN was selectively functionalized with poly(lactic acid) (PLA).[7] The PLA layer acted as a gatekeeper controlling the diffusion of neurotransmitters to the inside of the pores where they reacted with the surface-anchored OPTA groups. We found that several natural neurotransmitters, such as dopamine and glutamic acid, with different pK_a values indeed exhibited different fluorescence responses while interacting with the OPTA-MSN, indicating that it is possible to achieve a high degree of selectivity by controlling the diffusional penetration of analytes into the mesopores.[7] We demonstrated that the electrostatic, hydrogen bonding, and dipolar interactions between these neurotransmitters and the PLA layer in pH 7.4 buffer were the dominating factors in regulating the penetration of the neurotransmitters into the mesopores. In fact, at pH 7.4, dopamine is positively charged (pI = 9.7), whereas tyrosine and glutamic acid are negatively charged (pI $<$7.4). It has reported that PLA has an isoelectric point (pI) lower than 3.0 and is negatively charged in pH 7.4 buffer. The

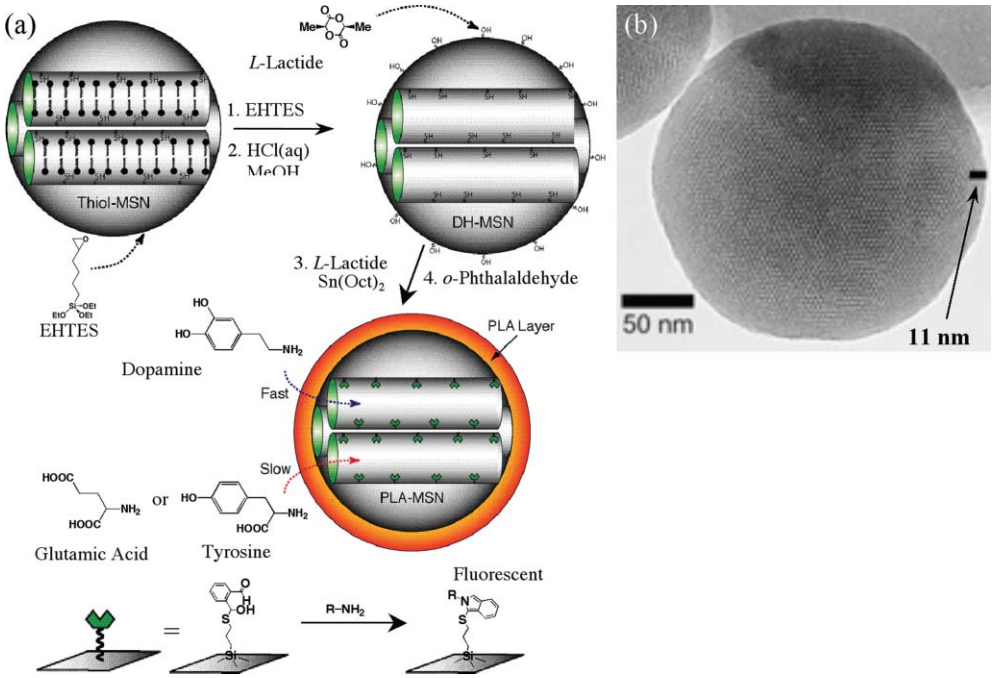

Fig. 11 (a) Schematic representation of the synthesis of PLA-coated MSN-based fluorescence sensor system for detection of amine-containing neurotransmitters, *i.e.*, dopamine, glutamic acid and tyrosine ($R–NH_2$) (EHTES =5,6-epoxyhexyltriethoxysilane); cetyltrimethylammonium bromide surfactant shown in schematic head–tail representation). (b) Transmission electron micrograph (TEM) of an ultramicrotomed PLA-MSN material. The layer of PLA can be visualized by the rim of amorphous structure surrounding the MCM-41 type of MSN core with mesopores packed in a hexagonal symmetry. Reprinted with permission from ref. 7. Copyright 2004, American Chemical Society.

neurotransmitters with attractive electrostatic characteristics to PLA (dopamine), had faster kinetics of entering the pores than those of the other neurotransmitters, such as glutamic acid, with repulsive forces.[7]

Another biosensor that was synthesized and studied by Martínez and co-workers involved aminomethylanthracene groups grafted onto MSNs and used for the recognition and detection of anions. The bulkiness of the grafted group combined with the steric restrictions provided by the pore size of the material led to the ability of the material to respond in different degrees to ATP, ADP and AMP (adenosine tri-, di-, and monophosphate, respectively). ATP was able to quench the fluorescence of the material to a larger degree than the other two species, and small anions such as chloride, bromide and phosphate did not produce any response of the sensor. They compared the sensitivity towards ATP of the amino-methylanthracene MSN with aminomethylanthracene grafted on fumed silica, and observed a 100-fold improved sensitivity when the matrix was mesoporous.[50,51]

Conclusion and outlook

This Feature Article describes in detail the recent progress of utilizing mesoporous silica nanomaterials as controlled release, drug delivery and biosensor systems. The studies reported here established the ability to load drugs and analytes into the mesopores and release by controlling the morphology and stimuli-responsiveness. The biosensors presented here are unique to MSN because of high porosity, which results in large surface areas available for the immobilization of the sensing molecules, and transparency, which permits optical detection even through the layers of the material itself. These two characteristics allows for low concentration detection and quick turnover.

As progress continues with the synthesis of different functional mesoporous nanomaterials, there is a need to tailor these novel materials for studying numerous avenues of biological systems. One such avenue is investigating selective endocytosis of functionalized MSN in mammalian and plant cells. If selective endocytosis is achieved then drugs may be delivered to selective cell types. Also, intracellular controlled release may be on the horizon, if biogenic molecules, such as drugs, genes and imaging agents, can be released by intra- or extra-cellular stimuli after selective endocytosis. Furthermore, if the pore sizes of MSN can be increased without altering the particle morphology and biocompatibility, the controlled release of therapeutic proteins, enzymes and large polynucleotides, can be achieved. Current state-of-the-art mesoporous silicas with large pore diameters, such as SBA-15 with 30 nm average pore diameter,[52] have particle size larger than 1 micron, which limit some biological applications. For example, cells cannot internalize such large particles. New research breakthroughs will foreseeably lead to new treatments for gene therapy, protein deficiencies, and metabolic disorders.

Acknowledgements

The authors thank the U.S. National Science Foundation (CHE-0239570) and the U.S. DOE Ames Laboratory (W-7405-Eng-82) for the support of their research.

References

1 J. S. Beck, J. C. Vartuli, W. J. Roth, M. E. Leonowicz, C. T. Kresge, K. D. Schmitt, C. T. W. Chu, D. H. Olson, E. W. Sheppard, S. B. McCullen, J. B. Higgins and J. L. Schlenker, *J. Am. Chem. Soc.*, 1992, **114**, 10834–10843.
2 Mesoporous Crystals and Related Nano-Structured Materials (Proceedings of the Meeting held 1–5 June 2004 in Stockholm, Sweden); ed. O. Terasaki, *Stud. Surf. Sci. Catal.*, 2004, **148.**
3 C.-Y. Lai, B. G. Trewyn, D. M. Jeftinija, K. Jeftinija, S. Xu, S. Jeftinija and V. S. Y. Lin, *J. Am. Chem. Soc.*, 2003, **125**, 4451–4459.
4 D. R. Radu, C.-Y. Lai, K. Jeftinija, E. W. Rowe, S. Jeftinija and V. S. Y. Lin, *J. Am. Chem. Soc.*, 2004, **126**, 13216–13217.
5 Y.-J. Han, G. D. Stucky and A. Butler, *J. Am. Chem. Soc.*, 1999, **121**, 9897–9898.
6 V. S. Y. Lin, C.-Y. Lai, J. Huang, S.-A. Song and S. Xu, *J. Am. Chem. Soc.*, 2001, **123**, 11510–11511.
7 D. R. Radu, C.-Y. Lai, J. W. Wiench, M. Pruski and V. S. Y. Lin, *J. Am. Chem. Soc.*, 2004, **126**, 1640–1641.
8 S. Jin and K. Ye, *Biotechnol. Prog.*, 2007, **23**, 32–41.
9 S. Radin, P. Ducheyne, T. Kamplain and B. H. Tan, *J. Biomed. Mater. Res.*, 2001, **57**, 313–320.
10 L.-X. Wen, H.-M. Ding, J.-X. Wang and J.-F. Chen, *J. Nanosci. Nanotechnol.*, 2006, **6**, 3139–3144.
11 Z. P. Xu, Q. H. Zeng, G. Q. Lu and A. B. Yu, *Chem. Eng. Sci.*, 2005, **61**, 1027–1040.
12 J.-F. Chen, H.-M. Ding, J.-X. Wang and L. Shao, *Biomaterials*, 2003, **25**, 723–727.
13 M. Vallet-Regi, A. Ramila, R. P. del Real and J. Perez-Pariente, *Chem. Mater.*, 2001, **13**, 308–311.
14 B. G. Trewyn, C. M. Whitman and V. S. Y. Lin, *Nano Lett.*, 2004, **4**, 2139–2143.
15 S. Giri, B. G. Trewyn, M. P. Stellmaker and V. S. Y. Lin, *Angew. Chem., Int. Ed.*, 2005, **44**, 5038–5044.
16 J. A. Gruenhagen, C.-Y. Lai, D. R. Radu, V. S. Y. Lin and E. S. Yeung, *Appl. Spectrosc.*, 2005, **59**, 424–431.
17 Y. W. Ebright, Y. Chen, Y. Kim and R. H. Ebright, *Bioconjugate Chem.*, 1996, **7**, 380–384.
18 V. L. Colvin, A. N. Goldstein and A. P. Alivisatos, *J. Am. Chem. Soc.*, 1992, **114**, 5221–5230.
19 A. Jeremic, K. Jeftinija, J. Stevanovic, A. Glavaski and S. Jeftinija, *J. Neurochem.*, 2001, **77**, 664–675.
20 E. A. Newman and K. R. Zahs, *Science (Washington, D.C.)*, 1997, **275**, 844–847.
21 J. E. Biaglow, J. Donahue, S. Tuttle, K. Held, C. Chrestensen and J. Mieyal, *Anal. Biochem.*, 2000, **281**, 77–86.
22 N. K. Mal, M. Fujiwara and Y. Tanaka, *Nature (London)*, 2003, **421**, 350–353.
23 D.-M. Huang, Y. Hung, B.-S. Ko, S.-C. Hsu, W.-H. Chen, C.-L. Chien, C.-P. Tsai, C.-T. Kuo, J.-C. Kang, C.-S. Yang, C.-Y. Mou and Y.-C. Chen, *FASEB J.*, 2005, **19**, 2014–2016.
24 Y.-S. Lin, C.-P. Tsai, H.-Y. Huang, C.-T. Kuo, Y. Hung, D.-M. Huang, Y.-C. Chen and C.-Y. Mou, *Chem. Mater.*, 2005, **17**, 4570–4573.
25 I. Slowing, B. G. Trewyn and V. S. Y. Lin, *J. Am. Chem. Soc.*, 2006, **128**, 14792–14793.
26 R. Hernandez, H.-R. Tseng, J. W. Wong, J. F. Stoddart and J. I. Zink, *J. Am. Chem. Soc.*, 2004, **126**, 3370–3371.
27 T. D. Nguyen, H.-R. Tseng, P. C. Celestre, A. H. Flood, Y. Liu, J. F. Stoddart and J. I. Zink, *Proc. Natl. Acad. Sci. USA*, 2005, **102**, 10029–10034.
28 T. D. Nguyen, Y. Liu, S. Saha, K. C. F. Leung, J. F. Stoddart and J. I. Zink, *J. Am. Chem. Soc.*, 2007, **129**, 626–634.
29 K. C. F. Leung, T. D. Nguyen, J. F. Stoddart and J. I. Zink, *Chem. Mater.*, 2006, **18**, 5919–5928.
30 T. D. Nguyen, K. C. F. Leung, M. Liong, C. D. Pentecost, J. F. Stoddart and J. I. Zink, *Org. Lett.*, 2006, **8**, 3363–3366.
31 S. G. Ansari, P. Boroojerdian, S. K. Kulkarni, S. R. Sainkar, R. N. Karekar and R. C. Aiyer, *J. Mater. Sci.: Mater. Electron.*, 1996, **7**, 267–270.
32 J. L. Besombes, S. Cosnier, P. Labbe and G. Reverdy, *Anal. Chim. Acta*, 1995, **317**, 275–280.
33 J. Wang and J. Liu, *Anal. Chim. Acta*, 1993, **284**, 385–391.
34 A. E. Ostafin, J. P. Burgess and H. Mizukami, *Tissue Eng. Novel Delivery Syst.*, 2004, 483–503.
35 B. M. Cullum and T. Vo-Dinh, *Biomed. Photonics Handb.*, 2003, **60**, 61–60.
36 D. Shan, M. Zhu, H. Xue and S. Cosnier, *Biosens. Bioelectron.*, 2007, **22**, 1612–1617.
37 S. Zong, Y. Cao, Y. Zhou and H. Ju, *Langmuir*, 2006, **22**, 8915–8919.
38 W. Shan, T. Yu, B. Wang, J. Hu, Y. Zhang, X. Wang and Y. Tang, *Chem. Mater.*, 2006, **18**, 3169–3172.
39 B. C. Dave, B. Dunn, J. S. Valentine and J. I. Zink, *Anal. Chem.*, 1994, **66**, 1120A–1127A.
40 J. I. Zink, S. A. Yamanaka, L. M. Ellerby, J. S. Valentine, F. Nishida and B. Dunn, *J. Sol–Gel Sci. Technol.*, 1994, **2**, 791–795.
41 R. Zusman, C. Rottman, M. Ottolenghi and D. Avnir, *J. Non-Cryst. Solids*, 1990, **122**, 107–109.
42 T. Coradin, M. Boissiere and J. Livage, *Curr. Med. Chem.*, 2006, **13**, 99–108.
43 J. H. Moon, W. McDaniel and L. F. Hancock, *J. Colloid Interface Sci.*, 2006, **300**, 117–122.
44 H. Yang and Y. Zhu, *Talanta*, 2006, **68**, 569–574.
45 S. R. Corrie, G. A. Lawrie and M. Trau, *Langmuir*, 2006, **22**, 2731–2737.
46 Y. Wei, H. Dong, J. Xu and Q. Feng, *ChemPhysChem*, 2002, **3**, 802–808.
47 J. L. Blin, C. Carteret, L. Rodehuser, C. Selve and M. J. Stebe, *Chem. Mater.*, 2005, **17**, 1479–1486.
48 Z. Dai, S. Liu, H. Ju and H. Chen, *Biosens. Bioelectron.*, 2004, **19**, 861–867.
49 Z. Dai, X. Xu and H. Ju, *Anal. Biochem.*, 2004, **332**, 23–31.
50 A. B. Descalzo, D. Jimenez, M. D. Marcos, R. Martinez-Manez, J. Soto, J. El Haskouri, C. Guillem, D. Beltran, P. Amoros and M. V. Borrachero, *Adv. Mater. (Weinheim, Germany)*, 2002, **14**, 966–969.
51 A. B. Descalzo, M. D. Marcos, R. Martinez-Manez, J. Soto, D. Beltran and P. Amoros, *J. Mater. Chem.*, 2005, **15**, 2721–2731.
52 D. Zhao, J. Feng, Q. Huo, N. Melosh, G. H. Frederickson, B. F. Chmelka and G. D. Stucky, *Science (Washington, D. C.)*, 1998, **279**, 548–552.